Mineralogical Magazine (2022), **86**, 903–909
doi:10.1180/mgm.2022.102

Article

New data on melanostibite, $Mn_2Fe^{3+}Sb^{5+}O_6$

Silvia Musetti[1]*, Cristian Biagioni[1,2], Ulf Hålenius[3], Elena Bonaccorsi[1,2] and Federica Zaccarini[4]

[1]Dipartimento di Scienze della Terra, Università di Pisa, Via Santa Maria 53, 56126 Pisa, Italy; [2]CISUP, Centro per l'Integrazione della Strumentazione dell'Università di Pisa, Pisa, Italy; [3]Department of Geosciences, Swedish Museum of Natural History, Box 50007, SE-10405, Stockholm, Sweden and [4]Physical and Geological Sciences, Faculty of Science, Universiti Brunei Darussalam, Jalan Tungku Link, Gadong BE1410, Bandar Seri Begawan, Brunei Darussalam

Abstract

Following the identification of a new occurrence of melanostibite from the Apuan Alps, the crystal chemistry of this mineral has been re-examined using specimens from its type locality, Sjögruvan, Örebro County, Sweden, and from the new occurrence, the Scortico–Ravazzone Mn ore deposit, Apuan Alps, Tuscany, Italy. Both specimens were examined through electron microprobe analysis, micro-Raman spectroscopy and single-crystal X-ray diffraction data; Mössbauer spectroscopy was used for the Swedish specimen. Electron microprobe data indicate a close to ideal composition $Mn_2Fe^{3+}Sb^{5+}O_6$ for both samples, whereas Mössbauer spectroscopy confirmed the trivalent oxidation state of Fe. Single-crystal X-ray diffraction for the Swedish and Italian specimens points to the acentric nature of melanostibite, space group *R*3. Refined unit-cell parameters of melanostibite from Scortico–Ravazzone and Sjögruvan are $a = 5.2351(3)$, $c = 14.3645(8)$ Å, $V = 340.93(4)$ Å^3, and $a = 5.2314(2)$, $c = 14.3518(8)$ Å, $V = 340.15(3)$ Å^3, respectively. Melanostibite is an homeotypic derivative of pyrophanite.

Keywords: melanostibite, crystal structure, manganese, iron, antimony, Sjögruvan, Sweden, Scortico-Ravazzone, Italy

(Received 21 July 2022; accepted 15 August 2022; Accepted Manuscript published online: 26 August 2022; Associate Editor: Peter Leverett)

Introduction

The hematite-type structure occurs in a series of important compounds and was one of the first structures to be solved (Pauling and Hendricks, 1925). It is characterised by hexagonal close packing (*hcp*) of anions, with cations occupying ⅔ of octahedral cavities. Four minerals are isotypic with hematite: corundum and the rare mineral species eskolaite, karelianite and tistarite (Table 1). These minerals have space group $R\bar{3}c$. The heterovalent substitution $2Me^{3+} = Me^{2+} + Ti^{4+}$ lowers the symmetry to $R\bar{3}$, as observed in the ilmenite-group minerals (Table 1). The very rare mineral melanostibite is related to pyrophanite, an ilmenite-group mineral, through the coupled substitution $2Ti^{4+} = Fe^{3+} + Sb^{5+}$. This mineral was first reported by Igelström (1893) from Sjögruvan, Örebro County, Sweden, under the name 'melanostibian' and later renamed melanostibite by Moore (1968a). Moore (1968a) demonstrated the relations between the ilmenite-group minerals and melanostibite, hypothesising that an ordered distribution of Fe^{3+} and Sb^{5+} may lower the symmetry to *R*3. However, the refinement of the crystal structure by Moore (1968b) suggested the possible $R\bar{3}$ space group, with a disordered distribution of Fe^{3+} and Sb^{5+}. Since then, the crystal structure of melanostibite (as well as of its synthetic counterpart $Mn_2Fe^{3+}Sb^{5+}O_6$) was assumed as centrosymmetric and all the following investigations dealing with the study of its ferroelectric and ferromagnetic properties, showing potential technological applications, were based on Moore's structural model (e.g. Hudl *et al.*, 2013; Mathieu *et al.*, 2013; Dos santos-García *et al.*, 2017; Liu *et al.*, 2019).

Recently, a new occurrence of melanostibite was identified in the Scortico–Ravazzone Mn ore deposit, Apuan Alps, Tuscany, Italy. Single-crystal X-ray diffraction studies indicated the probably acentric nature of the Italian sample, suggesting the opportunity to undertake a re-examination of this species also using material from the Swedish type locality. Moreover, new electron microprobe and spectroscopic data were collected, improving the knowledge on this very rare but technologically interesting compound.

Experimental

Specimens studied

Two specimens of melanostibite were available for this study. The first one was collected by one of us (C.B.) in the dumps of the Scortico–Ravazzone Mn ore deposit, Apuan Alps, Tuscany, Italy, briefly exploited during the 1940s. Melanostibite occurs as euhedral pseudohexagonal tabular crystals, reddish-black in colour, up to 0.1 mm in size, associated with Mn-rich carbonates, rhodonite, baryte and sarkinite (Fig. 1). Other minerals occur in this assemblage and a study of the mineralogy of this small ore deposit is currently underway. The other specimen is from the type locality, Sjögruvan, Örebro County, Sweden and is housed in the Swedish Museum of Natural History under catalogue number GEO-NRM #18890293. Melanostibite occurs as thin mm-sized black platelets associated with hausmannite, dolomite and katoptrite in cross-cutting fissures in metamorphosed limestone.

*Author for correspondence: Silvia Musetti, Email: silvia.musetti@dst.unipi.it
Cite this article: Musetti S., Biagioni C., Hålenius U., Bonaccorsi E. and Zaccarini F. (2022) New data on melanostibite, $Mn_2Fe^{3+}Sb^{5+}O_6$. *Mineralogical Magazine* **86**, 903–909. https://doi.org/10.1180/mgm.2022.102

Table 1. Hematite isotypic and homeotypic minerals.

Mineral	Chemistry	*a* (Å)	*c* (Å)	s.g.	Reference
Hematite group					
Corundum	Al_2O_3	4.75	12.99	$R\bar{3}c$	[1]
Eskolaite	Cr_2O_3	4.97	13.60	$R\bar{3}c$	[2]
Hematite	Fe_2O_3	5.04	13.77	$R\bar{3}c$	[3]
Karelianite	V_2O_3	4.95	14.00	$R\bar{3}c$	[4]
Tistarite	Ti_2O_3	5.15	13.64	$R\bar{3}c$	[4]
Ilmenite group					
Akimotoite	$MgSiO_3$	4.73	13.56	$R\bar{3}c$	[5]
Ecandrewsite	$ZnTiO_3$	5.09	13.99	$R\bar{3}c$	[6]
Geikielite	$MgTiO_3$	5.06	13.90	$R\bar{3}c$	[7]
Hemleyite	$FeSiO_3$	4.75	13.66	$R\bar{3}c$	[8]
Ilmenite	$FeTiO_3$	5.09	14.09	$R\bar{3}c$	[9]
Pyrophanite	$MnTiO_3$	5.13	14.25	$R\bar{3}c$	[6]
Melanostibite	$Mn_2Fe^{3+}Sb^{5+}O_6$	5.23	14.36	$R3$	[10]

[1] Ishizawa *et al.* (1980); [2] Logvinova *et al.* (2008); [3] Blake *et al.* (1966); [4] Newnham and de Haan (1962); [5] Horiuchi *et al.* (1982); [6] Mitchell and Liferovich (2004); [7] Liferovich and Mitchell (2006); [8] Bindi *et al.* (2017); [9] Wechsler and Prewitt (1984); [10] this work. s.g. = space group.

Chemical analysis

Quantitative chemical analyses were carried out using a Superprobe JEOL JXA 8200 electron microprobe ('Eugen F. Stumpfl' laboratory, Leoben University, Austria) using the following experimental conditions: wavelength dispersive spectroscopy mode, accelerating voltage = 20 kV, beam current = 10 nA and beam diameter = 1 µm. Counting times were 20 s on the peak and 10 s on the right and left backgrounds. Standards (element, emission line and diffracting crystals) were: magnetite (Fe*K*α, LIFH), stibnite (Sb*L*α, PETH) and rhodonite (Mn*K*α, LIFH). The contents of other sought elements with $Z > 8$ (including Ti) were below detection limits. Matrix correction by the ZAF method was applied to the data. Results are given in Table 2.

Mössbauer and micro-Raman spectroscopy

The ^{57}Fe Mössbauer spectrum of melanostibite from Sjögruvan, for which sufficient homogeneous material was available, was collected at room temperature in transmission mode using a ^{57}Co (in Rh matrix) point source, with a nominal activity of 0.40 GBq (Swedish Museum of Natural History, Stockholm, Sweden). Absorbers were prepared by gently grinding sample material (in the range 0.1–0.2 mg), which was placed in a ~2×2 mm square on a strip of tape and positioned closely in front of the point source. After calibrating the instrument against an α-Fe foil, the Mössbauer spectrum was acquired over the velocity range ±4 mm/s. The spectrum was fitted using the program *MossA* (Prescher *et al.*, 2012). Hyperfine parameters are given in Table 3.

Micro-Raman spectra of melanostibite were collected on both samples using a Horiba Jobin-Yvon XploRA Plus apparatus (Dipartimento di Scienze della Terra, Università di Pisa), with a 50× long-working-distance objective lens and the 532 nm line of a solid-state laser. The spectrum of the Italian sample was collected on the unpolished sample shown in Fig. 1, whereas data on the Swedish melanostibite were collected on the polished sample used for electron microprobe data. The latter gave a better spectrum that is shown in Fig. 3. This spectrum was collected through three acquisitions with single counting times of 120 s. Back-scattered radiation was analysed with a 1200 cm^{-1} grating monochromator.

Table 2. Chemical data for melanostibite and number of atoms per formula unit (apfu) based on O = 6 apfu.

	Scortico–Ravazzone			Sjögruvan		
	(*n* = 5)			(*n* = 15)		
Oxide	wt.%	range	e.s.d.	wt.%	range	e.s.d.
Sb_2O_5	42.68	42.28–43.06	0.36	42.34	41.57–42.84	0.36
MnO	36.73	36.49–36.94	0.19	36.37	36.10–37.43	0.32
Fe_2O_3	20.69	20.49–20.86	0.14	21.65	21.46–21.91	0.14
Total	100.13	99.89–100.53	0.25	100.36	99.56–101.07	0.38
apfu based on 6 O apfu						
Ti^{4+}	-	-	-	-	-	-
Sb^{5+}	1.02	1.00–1.02	0.01	1.00	0.98–1.00	0.01
Mn^{2+}	1.98	1.96–2.00	0.01	1.96	1.94–2.00	0.01
W^{6+}	-	-	-	-	-	-
Fe^{3+}	1.00	0.98–1.00	0.01	1.04	1.02–1.04	0.01

n = number of spot analyses. e.s.d. = estimated standard deviation.

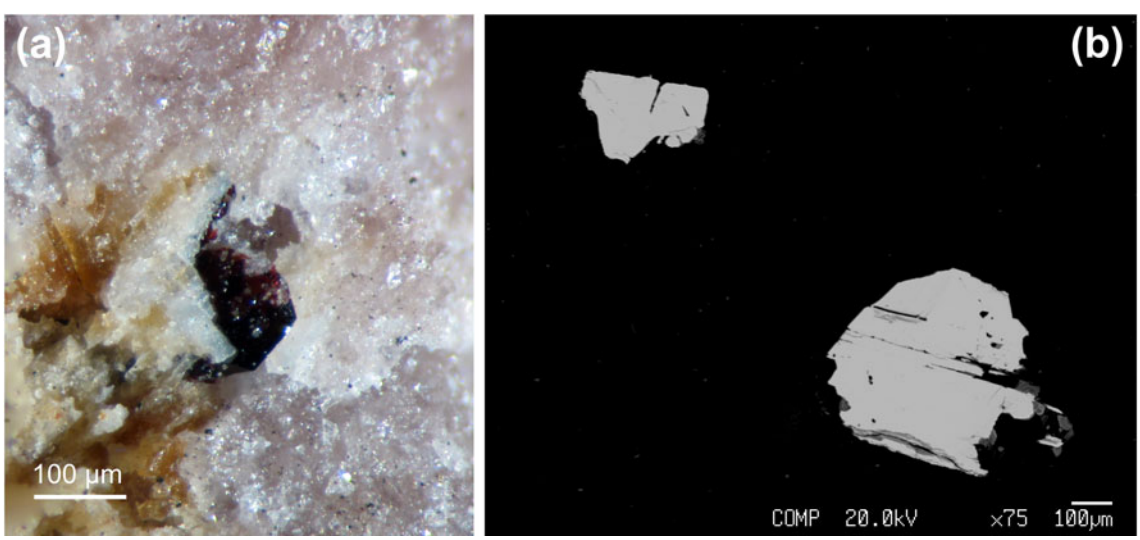

Fig. 1. Melanostibite. (a) Tabular pseudohexagonal crystal, dark red in colour, with Mn carbonates and silicates. Scortico–Ravazzone, Fivizzano, Massa-Carrara, Tuscany, Italy. Private collection, photo C. Biagioni. (b) Back-scattered electron image of melanostibite from Sjögruvan, Örebro County, Sweden.

https://doi.org/10.1180/mgm.2022.102 Published online by Cambridge University Press

Table 3. Mössbauer hyperfine parameters for melanostibite from Sjögruvan.

CS (mm/s)	QS (mm/s)	FWHM (mm/s)
0.376(5)	0.644(9)	0.303(12)

Note: CS = centre shift; QS = quadrupole splitting; FWHM = full width at half maximum.

Single-crystal X-ray diffraction and structural refinements

Single-crystal X-ray intensity data were collected on both samples of melanostibite. Data for the Italian sample were collected using a Bruker Apex II diffractometer (50 kV and 30 mA) equipped with a Photon II CCD detector and graphite-monochromatised Mo*K*α radiation (Dipartimento di Scienze della Terra, Università di Pisa, Italy). The detector-to-crystal distance was set at 50 mm. Data were collected using φ and ω scan modes in 0.5° slices, with an exposure time of 45 s per frame, and they were corrected for Lorentz, polarisation, absorption and background effects using the software package *Apex3* (Bruker AXS Inc., 2016). The Swedish specimen was studied using a Bruker D8 Venture diffractometer (50 kV and 1.4 mA) equipped with a Photon III CCD detector and monochromatised Mo*K*α radiation (Centro per l'Integrazione della Strumentazione scientifica dell'Università di Pisa, Università di Pisa, Italy). The detector-to-crystal distance was set at 38 mm. Data were collected using φ and ω scan modes in 0.5° slices, with an exposure time of 5 s per frame, and they were corrected for Lorentz, polarisation, absorption and background effects using the software package *Apex4* (Bruker AXS Inc., 2022). The statistical tests on the distribution of $|E|$ values gave $|E^2 - 1| = 0.589$ and 0.583 for the Italian and Swedish sample, respectively, thus suggesting the acentricity of melanostibite. Unit-cell parameters are $a = 5.2351(3)$, $c = 14.3645(8)$ Å and $V = 340.93(4)$ Å^3 for the sample from Scortico–Ravazzone, and $a = 5.2314(2)$, $c = 14.3518(8)$ Å and $V = 340.15(3)$ Å^3 for the specimen from Sjögruvan. In both cases, the space group is *R*3.

The crystal structure of melanostibite was solved through direct methods using *Shelxs-97* and refined using *Shelxl-2018* (Sheldrick, 2015). The following neutral scattering curves, taken from the *International Tables for Crystallography* (Wilson, 1992) were used: Sb *vs.* Fe at the *M*(1) and *M*(3) sites; Mn at *M*(2) and *M*(4) sites; and O at O(1) and O(2) sites. In the Italian sample, the *M*(1) and *M*(3) sites were found fully occupied by Fe and Sb, respectively and their occupancy was fixed to one. Table 4 gives details of data collection and refinement.

Results and discussion

Chemical formula

Both samples of melanostibite have chemical compositions close to ideal. The empirical formula of the sample from Scortico–Ravazzone, recalculated on the basis of 6 O atoms per formula unit (apfu), is $Mn_{1.98}(Sb_{1.02}Fe_{1.00})O_6$. The sample from Sjögruvan has chemical composition $Mn_{1.96}(Fe_{1.04}Sb_{1.00})O_6$; possibly, very minor Fe^{2+} could occur, partially replacing Mn^{2+}.

Mössbauer and micro-Raman spectroscopy

The Mössbauer spectrum of the sample from Sjögruvan shows only one quadrupole doublet (CS = 0.38 mm/s and QS = 0.64 mm/s)

Table 4. Summary of crystal data and parameters describing data collection and refinement for melanostibite.

	Scortico–Ravazzone	Sjögruvan
Crystal data		
Crystal size (mm)	0.100 × 0.080 × 0.075	0.030 × 0.030 × 0.015
Cell setting, space group	Trigonal, *R*3	Trigonal, *R*3
a (Å)	5.2351(3)	5.2314(2)
b (Å)	5.2351(3)	5.2314(2)
c (Å)	14.3645(8)	14.3518(8)
V (Å^3)	340.93(4)	340.15(3)
Z	3	3
Data collection and refinement		
Radiation, wavelength (Å)	Mo*K*α, λ = 0.71073	Mo *K*α, λ = 0.71073
Temperature (K)	293(2)	293(2)
$2\theta_{max}$ (°)	52.89	65.03
Measured reflections	1111	3082
Unique reflections	309	549
Reflections with $F_o > 4\sigma(F_o)$	309	549
R_{int}	0.0261	0.0296
$R\sigma$	0.0230	0.0223
Range of *h*, *k*, *l*	$-6 \le h \le 6$, $-6 \le k \le 6$, $-15 \le l \le 18$	$-6 \le h \le 7$, $-7 \le k \le 7$, $-21 \le l \le 21$
R [$F_o > 4\sigma(F_o)$]	0.0136	0.0128
R (all data)	0.0136	0.0128
wR (on F_o^2)	0.0311	0.0286
Goof	1.051	1.055
Flack parameter[2]	0.36(9)	0.92(6)
Number of least-squares parameters	33	34
Maximum and minimum residual peak (*e* Å^{-3})	+0.48 [at 0.98 Å from *O*(1)] −0.41 [at 0.84 Å from *M*(3)]	+0.56 [at 0.78 Å from *M*(3)] −0.61 [at 0.61 Å from *M*(4)]

[1]$w = 1/[\sigma^2(F_o^2)+(0.0159P)^2]$; $1/[\sigma^2(F_o^2)+(0.0159P)^2+0.6772P]$;
[2]Flack (1983)

https://doi.org/10.1180/mgm.2022.102 Published online by Cambridge University Press

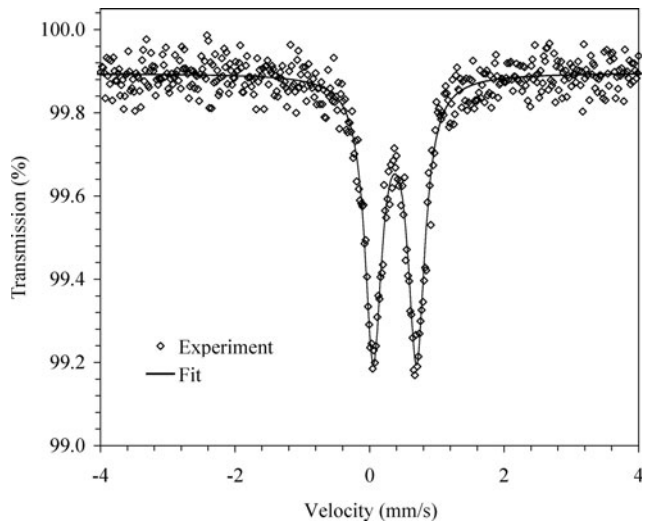

Fig. 2. Mössbauer spectrum of melanostibite from Sjögruvan.

related to the occurrence of Fe^{3+} (Fig. 2). This is in agreement with the occurrence of Fe at a single site. The value of the centre shift suggests that Fe^{3+} occurs at a six-coordinated site.

The micro-Raman spectra of melanostibite from Sjögruvan is shown in Fig. 3. The strongest bands occur between 550 and 700 cm^{-1}, probably related to the symmetrical stretching of Fe–O and Sb–O bonds. Moreover, the band at 678 cm^{-1} can be assigned to Mn–O symmetric stretching modes, in agreement with Kharkwal *et al.* (2010). It is worth noting that in pyrophanite, as well as in other ilmenite-group minerals, only two bands occur in this spectral region (e.g. Ross and McMillan, 1984; Okada *et al.*, 2008; Kharkwal *et al.*, 2010), whereas three distinct bands can be identified in melanostibite. Dos santos-García *et al.* (2017) reported the Raman spectrum of synthetic Mn_2FeSbO_6, which looks very similar to that observed for its natural counterpart. However, in the Supporting Information of their work, these authors gave only two bands, at 594 and 663 cm^{-1}, although a shoulder can be seen in their figure S7 that probably corresponds to the 678 cm^{-1} band observed in our study. Bands between 350 and 600 cm^{-1} can be attributed to bending vibrations of (Fe/Sb)-centred octahedra (e.g. Okada *et al.*, 2008; Dos santos-García *et al.*, 2017). Bands in the region below 350 cm^{-1} are probably related to lattice vibrations.

Crystal structure description

Fractional atomic coordinates and equivalent isotropic displacement parameters for melanostibite are given in Table 5, selected bond distances in Table 6 and bond-valence sums in Table 7. The crystallographic information files have been deposited with the Principal Editor of *Mineralogical Magazine* and are available as Supplementary material (see below).

Melanostibite is homeotypic with ilmenite, and can be described as an *hcp* of O atoms with cations occupying ⅔ of the octahedral cavities. In the crystal structure there are four independent cation sites, namely *M*(1)–*M*(4), and two O sites: O(1) and O(2). Manganese is hosted at the *M*(2) and *M*(4) sites; average bond distances are 2.214 and 2.209 Å in the Italian sample, and 2.216 and 2.206 Å for the Swedish sample. Moore (1968b) reported an average bond distance of 2.209 Å for the Mn site of melanostibite, with values ranging from 2.110 to 2.309 Å. The observed values are in accord with the ideal <Mn^{2+}–O> distance of 2.21 Å calculated using the ionic radii of $^{VI}Mn^{2+}$ and $^{IV}O^{2-}$

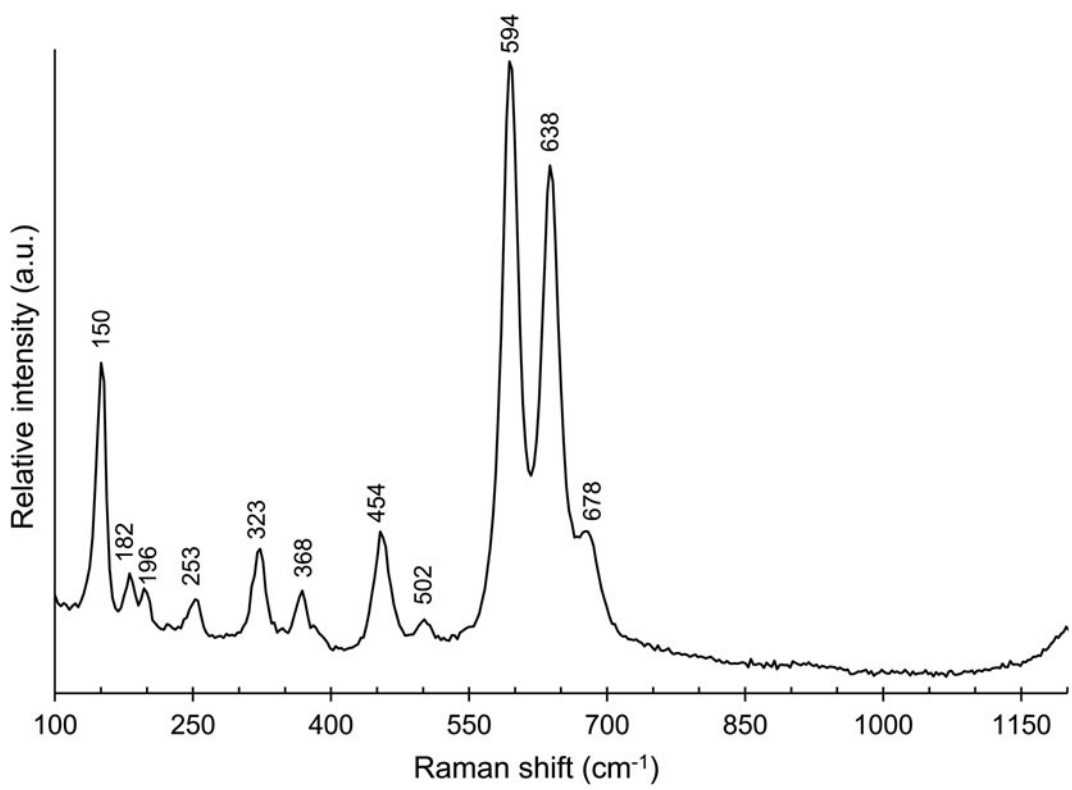

Fig. 3. Micro-Raman spectrum of melanostibite from Sjögruvan.

https://doi.org/10.1180/mgm.2022.102 Published online by Cambridge University Press

Table 5. Sites, Wyckoff positions, site occupancy factors (s.o.f.), fractional atom coordinates and equivalent isotropic displacement parameters (Å^2) for melanostibite.

Site	Wyckoff position	s.o.f.	*x/a*	*y/b*	*z/c*	U_{eq}
Scortico–Ravazzone						
M(1)	3*a*	$Fe_{1.00}$	0	0	0.18807(13)	0.0066(6)
M(2)	3*a*	$Mn_{1.00}$	⅓	⅔	0.36914(14)	0.0063(6)
M(3)	3*a*	$Sb_{1.00}$	⅓	⅔	0.15879(5)	0.0050(3)
M(4)	3*a*	$Mn_{1.00}$	0	0	0.9781(3)	0.0104(12)
O(1)	9*b*	$O_{1.00}$	0.9809(12)	0.6937(13)	0.5817(5)	0.0081(13)
O(2)	9*b*	$O_{1.00}$	0.2907(13)	0.9714(12)	0.0926(4)	0.0057(13)
Sjögruvan						
M(1)	3*a*	$Fe_{0.981(6)}Sb_{0.019(6)}$	0	0	0.18999(6)	0.0063(3)
M(2)	3*a*	$Mn_{1.00}$	⅓	⅔	0.37094(7)	0.0078(3)
M(3)	3*a*	$Sb_{0.949(8)}Fe_{0.051(8)}$	⅓	⅔	0.16086(2)	0.00509(11)
M(4)	3*a*	$Mn_{1.00}$	0	0	0.97972(9)	0.0095(4)
O(1)	9*b*	$O_{1.00}$	0.9812(6)	0.2891(8)	0.5838(2)	0.0076(6)
O(2)	9*b*	$O_{1.00}$	0.2907(7)	0.3198(6)	0.09482(19)	0.0078(6)

given by Shannon (1976). In addition, bond-valence sums agree with the occurrence of Mn^{2+}. Layers made by Mn-centred *M*(2) and *M*(4) octahedra alternate along **c** with ordered layers formed by Fe^{3+}- and Sb^{5+}-centred *M*(1) and *M*(3) octahedra (Fig. 4).

Whereas the bonding environments of the *M*(2) and *M*(4) sites of melanostibite described in this work are very similar to the coordination of the *Mn* site of the crystal structure reported by Moore (1968b), interesting differences can be observed for the *M*(1) and *M*(3) sites. Indeed, in the $R\bar{3}$ structural model only one (Sb/Fe) site occurs, with average bond distance of 2.008 Å and single bonds ranging from 1.967 to 2.049 Å. Using the ionic radii given by Shannon (1976), ideal <Fe^{3+}–O> and <Sb^{5+}–O> distances of 2.025 and 1.980 Å, respectively, can be calculated. The value observed by Moore (1968b) corresponds to a mixed ($Fe^{3+}_{0.5}Sb^{5+}_{0.5}$) site. In the *R*3 structure model, two symmetry-independent sites, namely *M*(1) and *M*(3) are present. The former has average bond distance ≈ 2.04 Å, whereas the latter shows an average distance of 1.99 Å. Such values, along with the refined site scattering, support an ordering of Fe^{3+} at the *M*(1) site and Sb^{5+} at the *M*(3) site, respectively. Bond-valence sums agree with such an ordering. Whereas the Italian sample shows pure Fe^{3+} and Sb^{5+} sites, the *M*(1) and *M*(3) sites of melanostibite from Sjögruvan seem to show a minor replacement of Fe^{3+} by Sb^{5+} at the *M*(1) site and vice versa at the *M*(3) position. In Table 5, the refined site occupancy factors are given; however, the substitution mechanism $^{M(1)}Fe^{3+} + {}^{M(3)}Sb^{5+} = {}^{M(1)}Sb^{5+} + {}^{M(3)}Fe^{3+}$ is likely, owing to the necessity of maintaining the electrostatic balance. The site populations $^{M(1)}(Fe^{3+}_{0.97}Sb^{5+}_{0.03})$ and $^{M(3)}(Sb^{5+}_{0.97}Fe^{3+}_{0.03})$ are proposed for the calculation of bond-valence sums. The significance of these mixed site occupancies will be discussed below.

Oxygen atoms are four-fold coordinated; their bond-valence sums fully confirm the occurrence of O^{2-} at these positions.

The structural formula of melanostibite can thus be written as $^{M(2)}(Mn_{1.00})^{M(4)}(Mn_{1.00})^{M(1)}(Fe_{1.00})^{M(3)}(Sb_{1.00})O_6 = Mn_2Fe^{3+}Sb^{5+}O_6$ ($Z = 3$).

Ferric iron-Sb^{5+} disorder in melanostibite: a possible explanation

As discussed briefly in the Introduction, this study originated from the structural characterisation of a new finding of melanostibite from Italy, which suggested the acentric nature of this ilmenite-related mineral. When we studied the more abundant Swedish type material, a crystal of approximately 200 × 200 × 150 µm was examined through single-crystal X-ray diffraction. The collected data showed the occurrence of several individuals within the studied grain; however it was possible to collect data, refining the structure in the space group $R\bar{3}$ down to $R_1 = 0.0321$ for 102 unique reflections. Notwithstanding the $|E^2 - 1| = 0.577$, a reliable solution in the *R*3 space group was not obtained. A large number of systematic absence violations (1296, for a total of 1883 read reflections) suggested the

Table 6. Selected bond distances (Å) for melanostibite.

	Scortico–Ravazzone	Sjögruvan
M(1)–O(1) × 3	1.978(6)	1.974(3)
M(1)–O(2) × 3	2.109(4)	2.105(3)
<*M*(1)–O>	2.044	2.040
M(2)–O(2) × 3	2.097(6)	2.100(3)
M(2)–O(1) × 3	2.330(7)	2.331(4)
<*M*(2)–O>	2.214	2.216
M(3)–O(2) × 3	1.964(5)	1.958(3)
M(3)–O(1) × 3	2.019(6)	2.025(3)
<*M*(3)–O>	1.992	1.992
M(4)–O(1) × 3	2.122(7)	2.112(3)
M(4)–O(2) × 3	2.296(7)	2.301(3)
<*M*(4)–O>	2.209	2.206

Table 7. Weighted bond-valence sums (in valence units) for melanostibite.*

Site	*M*(1)	*M*(2)	*M*(3)	*M*(4)	Σanions	Theor.
Scortico–Ravazzone						
O(1)	$0.55^{\times 3\downarrow}$	$0.24^{\times 3\downarrow}$	$0.77^{\times 3\downarrow}$	$0.40^{\times 3\downarrow}$	1.96	2.00
O(2)	$0.39^{\times 3\downarrow}$	$0.42^{\times 3\downarrow}$	$0.86^{\times 3\downarrow}$	$0.26^{\times 3\downarrow}$	1.93	2.00
Σcations	2.82	1.98	4.89	1.98		
Theor.	3.00	2.00	5.00	2.00		
Sjögruvan						
O(1)	$0.57^{\times 3\downarrow}$	$0.24^{\times 3\downarrow}$	$0.86^{\times 3\downarrow}$	$0.41^{\times 3\downarrow}$	2.08	2.00
O(2)	$0.40^{\times 3\downarrow}$	$0.42^{\times 3\downarrow}$	$0.74^{\times 3\downarrow}$	$0.26^{\times 3\downarrow}$	1.82	2.00
Σcations	2.91	1.98	4.80	2.01		
Theor.	3.06	2.00	4.94	2.00		

*Note: right superscripts indicate the number of equivalent bonds involving cations. The following site populations were used: Scortico–Ravazzone *M*(1) = Fe^{3+}, *M*(2) = Mn^{2+}, *M*(3) = Sb^{5+} and *M*(4) = Mn^{2+}; Sjögruvan *M*(1) = $Fe^{3+}_{0.97}Sb^{5+}_{0.03}$, *M*(2) = Mn^{2+}, *M*(3) = $Sb^{5+}_{0.97}Fe^{3+}_{0.03}$ and *M*(4) = Mn^{2+}. Bond valence units were calculated using the bond parameters of Gagné and Hawthorne (2015).

https://doi.org/10.1180/mgm.2022.102 Published online by Cambridge University Press

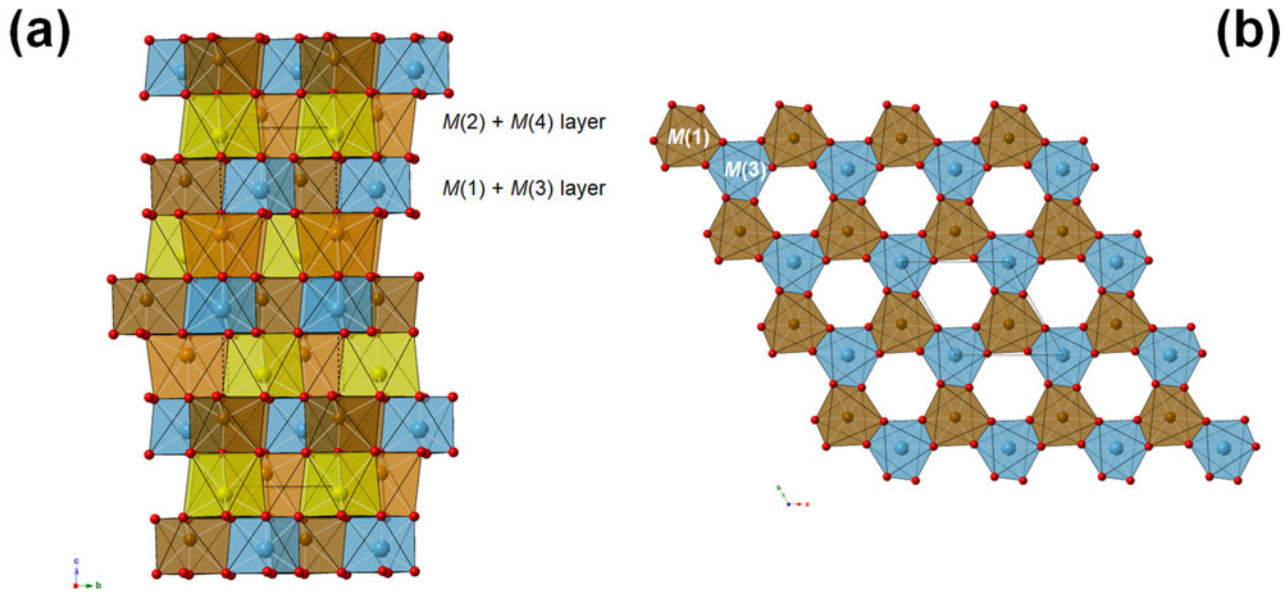

Fig. 4. Crystal structure of melanostibite: (a) as seen down **a**; and (b) details of the ordered $M(1)+M(3)$ layer as seen down **c**.

opportunity to examine better crystals. Indeed, Moore (1968b) highlighted his difficulty in finding crystals suitable for single-crystal X-ray diffraction, because "*most of the crystals were found to be not single but aggregates twinned by rotation on c {0001}*" (Moore, 1968b).

Using a smaller crystal (≈ 100 × 100 × 50 μm), better results were obtained. The crystal structure of melanostibite was refined in the space group *R*3 down to $R_1 = 0.0092$ for 512 unique reflections. No systematic absence violations were found. However, a partial disorder between Fe^{3+} and Sb^{5+} at the *M*(1) and *M*(3) sites was observed. The refined occupancies at these two sites were ($Sb_{0.62}Fe_{0.38}$) and ($Fe_{0.64}Sb_{0.36}$), respectively. This result was not in keeping with the Mössbauer data, that suggested a single Fe^{3+} site. However, the bond geometries of these two sites were very similar and could not be resolved through Mössbauer spectroscopy. *M*(1) and *M*(3) have average distances of 2.004 and 2.026 Å, with bond distances ranging between 1.96 and 2.05 Å at the *M*(1) site and 1.99 and 2.07 Å at the *M*(3) site. If structural data were correct, a possible hypothesis could be that melanostibite displays different degrees of Fe^{3+}–Sb^{5+} ordering, maybe as a result of crystallisation temperature or kinetics factors. However, the sample from the Italian locality was collected in a Mn ore deposit that experienced greenschist metamorphism (up to 350–450°C and 0.4–0.8 GPa at the metamorphic peak – Molli *et al.*, 2018 and references therein), and such values are probably not very different from the *P*–*T* conditions experienced by melanostibite from Sjögruvan. Holtstam and Mansfeld (2001) suggested an upper temperature limit of 470°C for the Sjögruvan deposit, and in addition they suggested that the hydothermal fissures at the deposit were formed in the temperature range 100–350°C.

Finally, using a microfocus source, we were able to collect data on a very small crystal (30 × 30 × 15 μm) of melanostibite from Sweden, and the structure was found to be acentric, with a very limited amount of Fe^{3+}–Sb^{5+} disorder between the *M*(1) and *M*(3) sites. As a relation between the size of the studied grains and the observed amount of Fe^{3+}–Sb^{5+} disorder was observed, we suggest that melanostibite is actually an ordered *R*3 ilmenite homeotype; the Fe^{3+}–Sb^{5+} mixed occupancy, as well as the apparent centrosymmetricity, probably result from the [0001] twinning and/or the possible occurrence of antiphase domains. Such kinds of defects are commonly reported in hematite- and ilmenite-type compounds (e.g. Tabata *et al.*, 1981; Lawson *et al.*, 1981; Hojo *et al.*, 2009) and can also be the reason for the widespread twinning reported by Moore (1968b).

Conclusion

Melanostibite is a homeotypic derivative of pyrophanite, with Fe^{3+} and Sb^{5+} ordered in two symmetry-independent octahedrally-coordinated sites. In addition to contributing to a better knowledge of this very rare (but technologically interesting) species, this investigation also stresses the important role of the study of regional mineralogy. Indeed, the finding of a new occurrence of melanostibite from a small and forgotten locality in the Apuan Alps promoted a reinvestigation of this species using modern analytical techniques, resulting in the discovery of the acentric nature of this long-known but poorly-characterised mineral species.

Acknowledgements. CB acknowledges financial support from the Ministero dell'Istruzione, dell'Università e della Ricerca through the project PRIN 2017 "TEOREM – deciphering geological processes using Terrestrial and Extraterrestrial ORE Minerals", prot. 2017AK8C32. CB and EB thank CISUP for the access to the single-crystal X-ray diffraction laboratory. The University Centrum for Applied Geosciences (UCAG) of the University of Leoben, Austria, is thanked for the access to the 'Eugen F. Stumpfl' electron microprobe Laboratory.

Supplementary material. To view supplementary material for this article, please visit https://doi.org/10.1180/mgm.2022.102

Competing interests. The authors declare none.

References

Bindi L., Chen M. and Xie X. (2017) Discovery of the Fe-analogue of akimotoite in the shocked Suizhou L6 chondrite. *Scientific Reports*, **7**, 42674.

Blake R.L., Hessevick R.E., Zoltai T. and Finger L.W. (1966) Refinement of the hematite structure. *American Mineralogist*, **51**, 123–129.

Bruker AXS Inc. (2016) *Apex3*. Bruker AXS Inc., Madison, Wisconsin, USA.

Bruker AXS Inc. (2022) *Apex 4*. Bruker AXS Inc., Madison, Wisconsin, USA.

Dos santos-García A.J., Solana-Madruga E., Ritter C., Andrada-Chacón A., Sánchez-Benítez J., Mompean F.J., Garcia-Hernandez M., Sáez-Puche R. and Schmidt R. (2017) Large magnetoelectric coupling near room temperature in synthetic melanostibite Mn_2FeSbO_6. *Angewandte Chemie*, **56**, 4438–4442.

Flack H.D. (1983) On enantiomorph-polarity estimation. *Acta Crystallographica*, **A39**, 876–881.

Gagné O.C. and Hawthorne F.C. (2015) Comprehensive derivation of bond-valence parameters for ion pairs involving oxygen. *Acta Crystallographica*, **B71**, 562–578.

Hojo H., Fujita K., Mizoguchi T., Hirao K., Tanaka I., Tanaka K. and Ikuhara Y. (2009) Magnetic properties of ilmenite-hematite solid-solution thin films: Direct observation of antiphase boundaries and their correlation with magnetism. *Physical Review*, **B80**, 075414.

Holtstam D. and Mansfeld J. (2001) Origin of a carbonate-hosted Fe-Mn-(Ba-As-Pb-Sb-W) deposit of Långban-type in central Sweden. *Mineralium Deposita*, **36**, 641–657.

Horiuchi H., Hirano M., Ito E. and Matsui Y. (1982) $MgSiO_3$ (ilmenite-type): single crystal X-ray diffraction study. *American Mineralogist*, **67**, 788–793.

Hudl M., Mathieu R., Nordblad P., Ivanov S.A., Bazuev G.V. and Lazor P. (2013) Investigation of the magnetic phase transition and magnetocaloric properties of the Mn_2FeSbO_6 ilmenite. *Journal of Magnetism and Magnetic Materials*, **331**, 193–197.

Igelström L.J. (1893) Melanostibian, ein neues Mineral von der Manganerzgrube Sjögrufvan, Kirchspiel Grythyttan, Gouvernement Örebro, Schweden. *Zeitschrift für Kristallographie und Mineralogie*, **21**, 246–248.

Ishizawa N., Miyata T., Minato I., Marumo F. and Iwai S. (1980) A structural investigation of α-Al_2O_3 at 2170 K. *Acta Crystallographica*, **B36**, 228–230.

Kharkwal M, Uma S. and Nagarajan R. (2010) Use of a chelating agent for the synthesis of high surface area pyrophanite $MnTiO_3$ powders. *Materials Letters*, **64**, 692–694.

Lawson C.A., Nord G.L., Dowty E. and Hargraves R.B. (1981) Antiphase domains and reverse thermoremanent magnetism in ilmenite-hematite minerals. *Science*, **213**, 1372–1374.

Liferovich R.P. and Mitchell R.H. (2006) The pyrophanite-geikielite solid-solution series: crystal structures of the $Mn_{1-x}Mg_xTiO_3$ series ($0 < x < 0.7$). *The Canadian Mineralogist*, **44**, 1099–1107.

Liu L., Song H.X., Li X., Zhang D., Mathieu R., Ivanov S., Skogby H. and Lazor P. (2019) Pressure-induced polymorphism and piezochroism in Mn_2FeSbO_6. *Applied Physics Letters*, **114**, 162903.

Logvinova A.M., Wirth R., Sobolev N.V., Seryotkin Y.V., Yefimova E.S., Floss C. and Taylor L.A. (2008) Eskolaite associated with diamond from the Udachnaya kimberlite pipe, Yakutia, Russia. *American Mineralogist*, **93**, 685–690.

Mathieu R., Ivanov S.A., Solovyev I.V., Bazuev G.V., Anil Kumar P., Lazor P. and Nordblad P. (2013) Mn_2FeSbO_6: A ferrimagnetic ilmenite and an antiferromagnetic perovskite. *Physical Review*, **B87**, 014408.

Mitchell R.H. and Liferovich R.P. (2004) The pyrophanite-ecandrewsite solid-solution: crystal structures of the $Mn_{1-x}Zn_xTiO_3$ series ($0.1 \leq x \leq 0.8$). *The Canadian Mineralogist*, **42**, 1871–1880.

Molli G., Vitale-Brovarone A., Beyssac O. and Cinquini I. (2018) RSCM thermometry in the Alpi Apuane (NW Tuscany, Italy): New constraints for the metamorphic and tectonic history of the inner northern Apennines. *Journal of Structural Geology*, **113**, 200–216.

Moore P.B. (1968a) Contributions to Swedish mineralogy. II. Melanostibite and manganostibite, two unusual antimony minerals. The identy of ferrostibian with långbanite. *Arkiv för Mineralogi och Geologi*, **4**, 449–458.

Moore P.B. (1968b) Substitutions of the type $(Sb^{5+}_{0.5}Fe^{3+}_{0.5})\leftrightarrow(Ti^{4+})$: the crystal structure of melanostibite. *American Mineralogist*, **53**, 1104–1109.

Newnham R.E. and de Haan Y.M. (1962) Refinement of the α Al_2O_3, Ti_2O_3, V_2O_3 and Cr_2O_3 structures. *Zeitschrift für Kristallographie*, **117**, 235–237.

Okada T., Narita T., Nagai T. and Yamanaka T. (2008) Comparative Raman spectroscopic study on ilmenite-type $MgSiO_3$ (akimotoite), $MgGeO_3$, and $MgTiO_3$ (geikielite) at high temperatures and high pressures. *American Mineralogist*, **93**, 39–47.

Pauling L. and Hendricks S.B. (1925) The crystal structures of hematite and corundum. *Journal of the American Chemical Society*, **47**, 781–790.

Prescher C., McCammon C. and Dubrovinsky L. (2012) MossaA: a program for analyzing energy-domain Mössbauer spectra from conventional and synchrotron sources. *Journal of Applied Crystallography*, **45**, 329–331.

Ross N.L. and McMillan P. (1984) The Raman spectrum of $MgSiO_3$ ilmenite. *American Mineralogist*, **69**, 719–721.

Shannon R.D. (1976) Revised effective ionic radii and systematic studies of interatomic distances in halides and chalcogenides. *Acta Crystallographica*, **A32**, 751–767.

Sheldrick G.M. (2015) Crystal Structure Refinement with SHELXL. *Acta Crystallographica*, **C71**, 3–8.

Tabata H., Ishii E. and Okuda H. (1981) Cation antiphase boundaries in ionic crystals based on anion close packing. *Journal of Crystal Growth*, **52**, 956–962.

Wechsler B.A. and Prewitt C.T. (1984) Crystal structure of ilmenite ($FeTiO_3$) at high temperature and pressure. *American Mineralogist*, **69**, 176–185.

Wilson A.J.C. (1992) *International Tables for Crystallography*. Volume C. Kluwer, Dordrecht, The Netherlands.